Extended Reception Coverage and Spoofing Localization of Direct Remote ID utilizing Ad-Hoc Mesh Networking

M. F. Høffer [1], V. D. Herlev[1], G. Maalouf[1], J. H. Jepsen[1], E. Winkler[1], I. Panov[2], and K. Jensen[1]
[1]SDU UAS Center, University of Southern Denmark, Odense
[2]Department of Business Development and Technology, Aarhus University, Aarhus

http://www.imavs.org/

ABSTRACT

Direct Remote Identification (DRI) identifies and localizes nearby Unmanned Aerial Vehicles (UAVs) by transmitting the location and identity of the UAV and operator via Bluetooth or Wi-Fi. As of 1 January 2024, the EU mandates remote identification for UAVs in category C. Current DRI systems have a limited range and lack digital signatures, making them vulnerable to spoofing.

This paper addresses the first limitation by using a Flying Ad-Hoc Network (FANET) to extend the range of DRI messages with a meshing algorithm. The second limitation is tackled by investigating RSSI localization methods. Spoofing detection is achieved by comparing estimated and broadcast locations. The meshed system was tested and reliably received messages at a 1.6 km range, previously unattainable. Localization experiments demonstrated the approximate localization of both static and moving DRI devices using a receiver network.

1 INTRODUCTION

As of 1 January 2024, the European Union's 2019/947 regulation [1] mandates that Unmanned Aerial Vehicles (UAVs) in category C use a modern remote identification system. Two modes exist: Network Remote Identification (NRI) is used within U-space airspace, while Direct Remote Identification (DRI) is used outside of U-space.

Both modes transmit operator and UAV information, but NRI broadcasts globally via the internet, while DRI broadcasts locally. Only DRI is required for operations outside U-space, allowing authorities and the public to receive information within a certain range through software applications.

The DRI standard [2] supports four wireless technologies: Bluetooth Legacy Advertising, Bluetooth Long Range, Wi-Fi Beacon, and Wi-Fi Neighbor Aware Network (NAN). These technologies have a limited range of a few hundred meters [3].

Moreover, the DRI standard lacks specifications for verifying message through digital signature. While the Internet Engineering Task Force is working on DRI security [4, 5], current specifications do not address this, making spoofing a significant threat to UAV situational awareness and airspace security. A malicious actor could transmit false DRI messages, evading detection or simulating one or more UAVs with a single transmitter.

The two weaknesses of the current DRI standard are illustrated in Fig. 1. The contribution of this work is to 1) demonstrate how the range of DRI can be increased with the use of mesh networking to create a Flying Ad-Hoc Network (FANET), and 2) investigate how a device transmitting fake DRI messages can be localized using a receiver network.

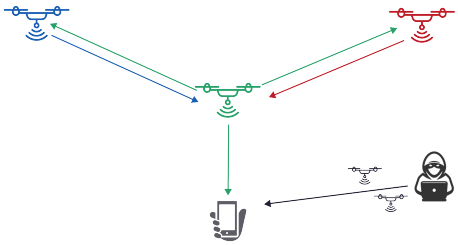


Figure 1: The green UAV is able to receive DRI messages from the blue and red UAV. However, the DRI scanner application only receives DRI messages from the green UAV. The blue and red UAV have no knowledge of each other. The system is vulnerable to spoofing devices.

The paper is organized as follows: Section 2 of the paper gives an overview of the state of the art with the field of ad-hoc mesh networks for UAVs and localization using wireless sensor network. Section 3 describes the architecture of the presented DRI FANET, including 1) how it extends the range of DRI messages (Section 3.1) and 2) how it localizes DRI spoofing devices (Section 3.2). The results are discussed in Section 4. Finally, Section 5 covers the conclusion and future work.

2 STATE OF THE ART

Ho et al. argues that flooding is a viable broadcasting algorithm for high reliability in very dynamic networks [6]. The argument is based on the fact that keeping accurate information of neighboring nodes is difficult for high-mobility nodes. Simulations are performed that visualize how the flooding algorithm performs in terms of the number of collisions, duplicate messages, and packet loss as a function of the node speed.

In [7], the difficulties related to broadcasting information in a mobile ad-hoc network are addressed. These concerns can be directly transferred to FANETs. The paper focuses on the broadcast storm problem, which is a collection of problems associated with flooding. To combat issues regarding

http://www.imavs.org/

redundancy, network congestion and packet collisions, the authors propose different broadcast algorithms such as probabilistic and location-based schemes, and analyze their performance.

In [8], the authors propose a solution to reduce broadcast redundancy in wireless mobile networks. The proposed solution is the Scalable Broadcast algorithm (SBA), which uses 2-hop neighbor information to make local decisions with very little overhead. Other neighbor knowledge methods exist, where the routing decision is not made locally but instead predetermined by the previous transmitter [9, 10].

Williams and Camp categorize and use simulation to compare different broadcasting algorithms usable in mobile ad-hoc networks [11]. The categories include simple flooding, probabilistic methods, area-based methods, and neighbor knowledge methods. In terms of redundant retransmissions of packets in dense networks, their results show that simple flooding performs the worst, while the neighbor knowledge methods perform the best. Additionally, they show that neighbor knowledge methods that do not make local decisions perform the worst in high mobility networks, in terms of packet delivery ratio.

Localization of Wireless Sensor Nodes (WSNs) is an active area of research as more wireless devices with a need for a location estimate enter the market [12]. A common approach in localization is to use anchor nodes that broadcast their known locations to estimate the position of other nodes [13]. In the context of DRI, the roles are instead reversed, as the goal is to localize a spoofing device based on the information the device itself transmits. Localization of WSNs can broadly be categorized in two categories; range-based and range-free localization [14]. Range-based localization methods utilize a distance or angle measurement between an unknown position and several anchor nodes with known positions.

Estimating the distance to anchor nodes is often done using the log-distance path loss model given that the received power, path loss exponent, and a reference received power at e.g $1\mathrm{m}$ is known[15, 16]. The main challenge in using the log-distance path loss model lies in estimating the path loss exponent, which is dependent on the environment. In [16] the path-loss exponent and reference received power are numerically estimated through a least squares minimization.

Blumental et.al proposes a range-based localization method called Weighted Centroid Localization (WCL) algorithm in [17]. Sensor nodes with unknown positions can estimate their position as a weighted sum of the anchor nodes' positions, where the weight is determined based on the distance between the sensor node and anchor nodes. In [18] a range-free extension of the WCL algorithm is proposed, the Weight Compensated Weighted Centroid Localization (WCWCL) algorithm, where the weights no longer rely on a distance measurement, but purely the signal strength. Simulation and experimental results show an improved localization accuracy compared to WCL.

3 DRI FLYING AD-HOC NETWORK (FANET)

The conceptional idea of presented DRI FANET is illustrated on Fig. 2. Each DRI device in the FANET is based on an XIAO ESP32-C3 development board [19], which is a suitable candidate for an embedded platform used in mesh network applications on UAVs due to the following reasons; it has both Bluetooth and Wi-Fi capabilities; it has an onboard battery circuit; it has a low price; the weight is $10\,\mathrm{g}$, and; it has the size of $21\,\mathrm{mm} \times 17.5\,\mathrm{mm}$. For further details, we refer to the Master's Thesis of M. F. Høffer and V. D. Herlev [20].

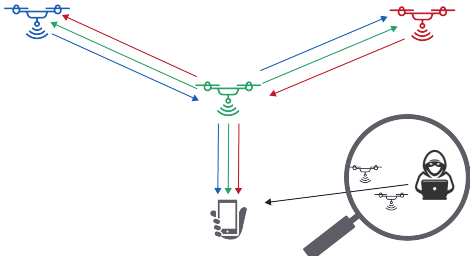


Figure 2: All UAVs are aware of each other and the DRI scanner application receives DRI messages from all UAVs. This is achieved by the green UAV forwarding messages from the others. Additionally, the spoofing devices are localized.

3.1 Extending the coverage range of DRI

The conceptual idea of extending the coverage range of the DRI is illustrated on Fig. 3, and is obtained by having individual nodes receive the DRI messages and retransmit them based on a forwarding rule. Since only broadcasting is considered, this rule will be determined by a broadcast algorithm. If the forwarding rule was to retransmit all packets blindly, the packets would be broadcast. However, the network would quickly become congested because of the packets moving in loops.

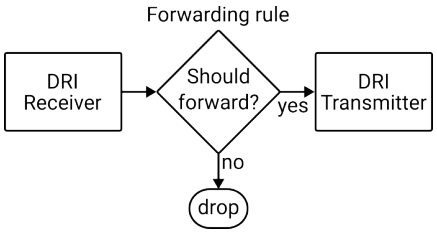


Figure 3: DRI ad-hoc mesh network principle. A DRI receiver listens for DRI messages, if the forwarding rule decides that the message should be forwarded, it is rebroadcast using the DRI transmitter, otherwise, it is dropped.

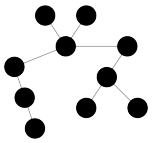


Figure 4: Sparse network where the structure can be described as a tree or a graph without cycles.

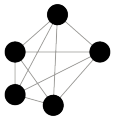


Figure 5: Dense fully connected network. Every node is connected to every other node.

3.1.1 Comparison of different broadcast algorithms

Table 1 summarizes the different broadcast algorithms that have been considered for the DRI FANET; In **simple flooding**, every node forwards every packet exactly once; The three probabilistic methods **counter-based**, **distance-based**, and **location-based** use a threshold value to determine whether to forward a packet; The two neighbor-based approaches, Scalable Broadcast Algorithm (SBA) and Ad-Hoc Broadcast Protocol (AHBP), use two-hop neighbor knowledge to determine whether to forward a packet, where: 1) In **SBA**, if a node has neighbors that are not covered already, it will rebroadcast the packet, and 2) In **AHBP** every node selects a list of Broadcast Relay Gateways (BRGs), which are the only nodes allowed to forward the packet. The BRGs are selected such that all nodes in the network will be covered by a broadcast. Some of the algorithms require attaching additional information to the DRI messages. Modification of DRI messages can result in standard receivers not being able to receive the forwarded message, which is not desirable.

In [11], Williams and Camp categorize and compare different broadcast algorithms in simulation. Their results show that the two probabilistic methods counter-based and location-based perform worst in dense networks (Fig. 5), while AHBP performs worse for networks with high mobility. Additionally, the probabilistic methods do not guarantee delivery in certain network topologies.

It is assumed that networks consisting of UAVs are sparse (Fig. 4) and have a highly dynamic topology, as the UAVs are expected to move. In this case, both SBA and simple flooding are applicable algorithms. However, SBA has increased overhead in keeping track of neighboring nodes. Additionally, SBA does not rebroadcast messages at the ends of branches and therefore has reduced coverage compared to simple flooding. For this reason, the simple flooding algorithm is chosen to extend the range of DRI.

3.1.2 Implementation

The simple flooding algorithm is implemented on the ESP32-C3 as illustrated on Fig. 6. Additionally, integration with a flight controller is achieved through MAVLink[21]. This makes the UAV aware of other UAVs on the network, as well as making other UAVs on the network aware of the UAV itself.

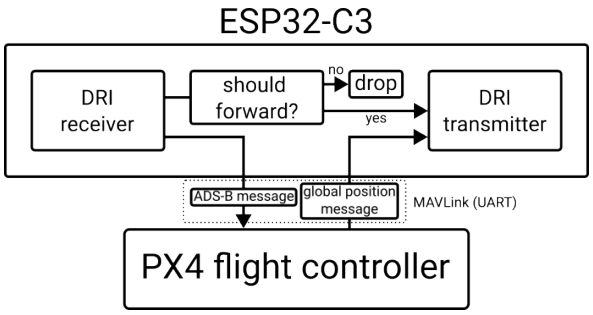


Figure 6: Integration of the DRI with a PX4-based flight controller for extending its coverage range using the simple flooding broadcast algorithm.

3.1.3 Results

The experimental validation of extending the DRI range is visualized on Fig. 7. The DRI FANET consists of eleven ESP32-C3s, each with the simple flooding broadcast mesh algorithm implemented.

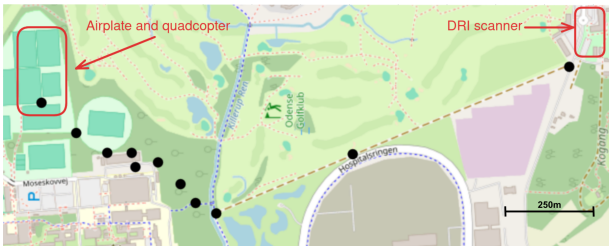


Figure 7: Location of relay nodes used for broadcast mesh network verification. AirPlate[22] and quadcopter are placed on one end of the chain and a DRI scanner on the other end. DRI messages transmitted by the Airplate and quadcopter will be forwarded through the chain of relay nodes using the developed broadcast algorithm.

Two PX4-based [23] flight controllers are used in the setup; One of the flight controllers is used for controlling a multirotor UAV that will be flying and transmitting DRI messages at 10Hz, and; One flight controller is connected to a Ground Control Station (GCS), used as a DRI scanner through QGroundControl[24]. Both flight controllers are communicating with an ESP32-C3 using the MAVLink protocol, as illustrated on Fig. 6. An AirPlate [22], a spinout from the GENIUS project [25] is used to verify that the FANET also supports devices without mesh network capabilities. The airline distance between the two ends of the relay chain is approximately 1.6 km. Fig. 8 shows the frequencies at which the messages from the quadcopter and AirPlate arrive at the DRI scanner. The altitude of the quadcopter is

http://www.imavs.org/

Algorithm	Can be implemented without modifying DRI?	Most applicable for sparse or dense network?	Handles networks with dynamic topology well?
Simple Flooding	Yes	Sparse	Yes
Counter-Based	Yes	Dense	Yes
Distance-Based	Yes	-	-
Location-Based	No	Dense	Yes
SBA	Yes	All	Yes
AHBP	No	All	No

Table 1: Comparison of different broadcast algorithms, where the properties relevant in the context of a DRI FANET are shown.

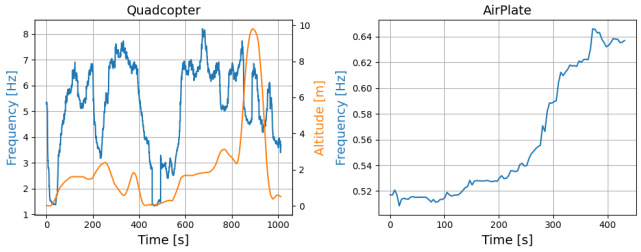


Figure 8: Moving average, with a window size of 150, of the frequency at which DRI messages arrive at the DRI scanner from the quadcopter and AirPlate respectively. The quadcopter broadcasts at 10 Hz, while the AirPlate broadcasts at 1 Hz.

plotted alongside the frequency, to show that the frequency is lowest when the quadcopter is on the ground.

The message frequency can be used as a measure for the delivery ratio, as it ideally should be 10 Hz and 1 Hz for the quadcopter and AirPlate respectively. To validate the implemented solution, it was verified that all of the messages arriving at the DRI scanner came from the last node in the relay chain exclusively. A video of the experiment can be found in [26].

3.2 Localization of a DRI spoofing device using FANET

As mentioned, the DRI specification does not implement any sort of verification of DRI messages. As a result of this, all of the information in the DRI messages could be spoofed. Figure 9 illustrates the potential issues that can arise from this vulnerability. This section investigates if it is possible to localize a device transmitting DRI messages. This can then be used to determine if a device is spoofing its position. Detecting if other information in the DRI messages is incorrect, such as the UAV and operator ID, is not considered.

One measurable metric that can be used for localization is the Received Signal Strength Indicator (RSSI). In the presented work, two localization methods based on RSSI measurements are evaluated; 1) Multilateration, a range-based RSSI localization method, and 2) Weight Compensated Weighted Centroid Localization (WCWCL), a range-free RSSI localization method.



Figure 9: Example of a single device spoofing HCA airport. Note that the experiment is performed in an isolated environment and therefore caused no impact on real-world air traffic.

3.2.1 Multilateration

Based on the log-distance path loss model, the distance between transmitter and receiver can be estimated using Eq. (1), where $\text{RSSI}(d_0)$ is a reference RSSI measurement made at a distance d_0 and n is the path loss exponent.

$$d = d_0 10^{\frac{\text{RSSI}(d_0)-\text{RSSI}(d)}{10n}} \tag{1}$$

In the context of DRI spoofing, there will be one transmitter and N receiver nodes. For each receiver node n_i with coordinates (x_i, y_i), a corresponding distance estimate d_i to the transmitter will be calculated. Each distance estimate will correspond to a circle with center (x_i, y_i) and radius d_i, that the transmitter can be located on. In an ideal case, the circles intersect at exactly one point (x, y) which can be determined analytically. Due to inaccuracies in the distance estimates this is however unlikely. If several anchor nodes $n > 3$ are used, an over-determined system of equations can be formulated as seen in Eq. (2).

$$\begin{aligned} (x-x_1)^2+(y-y_1)^2 &= d_1^2 \\ &\vdots \\ (x-x_n)^2+(y-y_n)^2 &= d_n^2 \end{aligned} \tag{2}$$

http://www.imavs.org/

http://www.imavs.org/

The system of equations can be represented on matrix form as $\boldsymbol{Ax} = \boldsymbol{b}$, which can be solved using Eq. (3), where $\hat{\boldsymbol{x}} = (\hat{x}, \hat{y})$ is the estimated transmitter position.

$$\hat{\boldsymbol{x}} = (\boldsymbol{A}^T\boldsymbol{A})^{-1}\boldsymbol{A}^T\boldsymbol{b} \tag{3}$$

3.2.2 WCWCL

Range-free localization does not rely on a distance measure, and therefore not on an estimate of the path loss exponent. In [18] a novel range-free localization algorithm, called Weight Compensated Weighted Centroid Localization (WCWCL), is presented. In WCWCL each anchor node in the receiver network is assigned a weight, which is calculated based on the RSSI value as shown in Eq. (4), where g is the degree that determines the contribution from each receiver node.

$$W_i = \frac{w_i}{\sum_{j=1}^{n} w_j} = \frac{\sqrt{\left(10^{\frac{RSSI_i}{10}}\right)^g}}{\sum_{j=1}^{n}\sqrt{\left(10^{\frac{RSSI_j}{10}}\right)^g}} \tag{4}$$

A weight compensated weight Wc_i is then calculated to increase the weight of receiver nodes that are closer to the transmitter, this is shown in Eq. (5), where n is the number of receiver nodes.

$$Wc_i = \frac{W_i \cdot n^{2W_i}}{\sum_{j=1}^{n}(W_j \cdot n^{2\cdot W_j})} \tag{5}$$

Based on the assigned weights the position of the transmitter P is then calculated as the sum of the product of the weights Wc_i and the position of each receiver node P_i, as shown in Eq. (6).

$$P = \sum_{j=1}^{n}(Wc_i \cdot P_i) \tag{6}$$



Figure 10: Receiver node with an ESP32-C3 and a 2.15 dBi stacked dipole whip antenna mounted on a bamboo stick, used in the localization experiment.

3.3 Results

3.3.1 Preliminary experiment

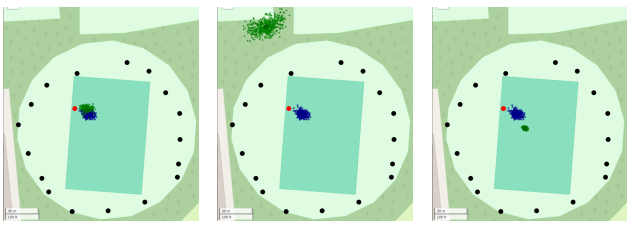
To evaluate the performance of the presented localization methods, a DRI receiver network of seventeen ESP32-C3s is used for the localization experiment. Each ESP32-C3 is equipped with 2.15dBi stacked dipole whip antennas [27] and is distributed in a circular area with known positions. One of the receivers can be seen on Fig. 10. For each experiment, 500 DRI messages are transmitted from a static known location. Three different experiments are conducted; 1) static RSSI localization experiment with its default transmissions power, 2) static RSSI localization experiment with different transmissions power, and 3) RSSI localization experiment while moving the spoofing device around.

Static RSSI localization experiment: The static RSSI localization experiment is performed in 15 different locations. The results from three of these can be seen on Fig. 11.



Figure 11: Receiver locations are in black, and the true transmitter location is in red. WCWCL estimates ($g = 1.5$) are shown in blue, and multilateration estimates ($n = 2$) in green. The mean estimate location is marked with larger green and blue icons.

Static RSSI localization experiment with changing transmission power: Assuming a spoofing device was present, a continuously varying transmitter power could be expected to simulate different locations. To simulate a transmitter device changing its output power, the RSSI measurements are manually offset with $\pm$5dB, as shown in Fig. 12.

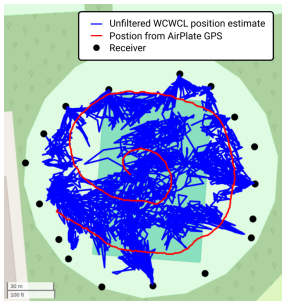


(a) Original RSSI measurements (b) -5dB from RSSI to simulating weaker transmitter (c) +5dB to RSSI simulating stronger transmitter

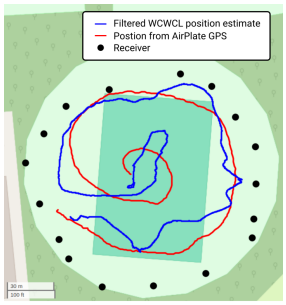
Figure 12: RSSI localization using whip antennas, showing the impact of changing transmitter power. Receiver locations are in black, true transmitter locations in red, WCWCL estimates ($g = 1.5$) in blue, and multilateration estimates ($n = 2$) in green. The mean location of estimates is marked with larger green and blue icons.

http://www.imavs.org/

Moving RSSI localization experiment: A final localization experiment was conducted while moving an AirPlate around. The experimental setup is identical to the previous two static experiments. The AirPlate is moved around in a spiral for 398 seconds while the position is logged through the transmitted DRI messages. The WCWCL position estimate and the global position from the AirPlate are plotted on Fig. 13a. A moving average with a window size of 200, corresponding to 20 seconds of data, is used to filter the position estimates as shown on Fig. 13b.



(a) Unfiltered WCWCL position estimate.



(b) Moving average of WCWCL position estimate.

Figure 13: Comparison of the logged GPS position of the AirPlate in red and the estimated position using WCWCL with $g = 1.8$ in blue. The receiver locations are visualized in black.

3.3.2 Real-world validation

To evaluate the practicality of the proposed solution in a real-world context, an experiment was conducted at the Danish national UAS test center, at Hans Christian Andersen Airport (HCAA), Odense, Denmark, where spoofing poses a potential security threat. For this experiment, eight DRID receivers configured to log DRID messages onto an SD card were deployed in a triangular arrangement on a small section of the airport fence, with a maximum separation of 150 meters between them. All receivers were equipped with 9dBi stacked dipole antennas. The DRID emitter used in this experiment was an AirPlate [22], which was mounted underneath a DJI Mini 4 Pro drone. The drone was flown around the airport at various altitudes to simulate different operational conditions. Figure 14 below illustrates the experimental setup.

To test the localization accuracy of the system, the drone was hovered for 15 seconds at altitudes of 25, 50, 75, and 100 meters, respectively. The results of those hover tests are presented in Table 2, and can be visualized in Figure 15. It can be seen from Table 2 that the mean error tends to increase at higher altitudes.

Additionally, the UAV was flown around the airport at a constant altitude to observe the system's behavior as the UAV crossed the boundary of the coverage area. As shown in Figure 16, when the UAV operates outside the coverage area,



(a) DRID receiver with 9dBi stacked dipole antenna, and SD logging capability.



(b) AirPlate DRID emitter mounted underneath the DJI Mini 4 Pro.



(c) Map of the location of the DRID receivers at the HCAA.

Figure 14: Real-world spoofing localisation experimental setup at HCA airport using eight DRID receivers, and an AirPlate DRID emitter mounted below a DJI Mini 4 Pro.

Table 2: Mean Error and Standard Deviation of Hover Test

Altitude	Mean Error	Standard Deviation
25 m	5.026 m	17.902 m
50 m	9.217 m	39.380 m
75 m	41.900 m	17.788 m
100 m	13.322 m	24.225 m

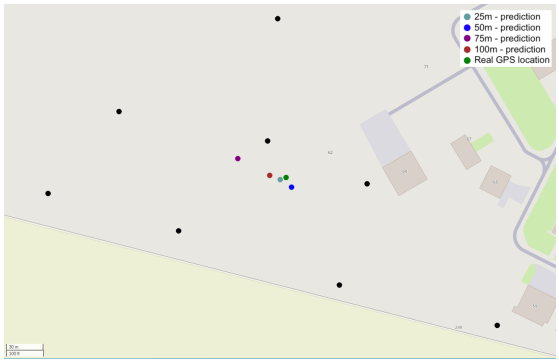


Figure 15: Localisation results from the experiment at altitudes of 25, 50, 75, and 100 meters. The colored dots represent the averaged localization predictions from the system, while the green dot indicates the true GPS location of the UAS at each altitude.

the predicted location is positioned at the edge of the coverage zone, leading to inaccurate localization. However, this prediction can still serve as a directional guide, assisting in narrowing down the search area outside the fence.

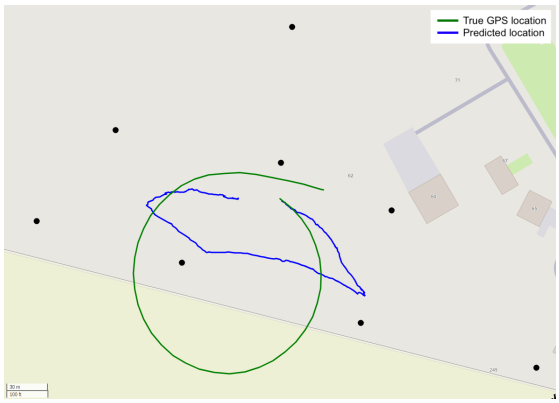


Figure 16: Localisation results as the UAS flies in a circle at a constant altitude crossing the boundary of the coverage area.

4 DISCUSSION

Theoretical Limits of the Broadcast Algorithm: The theoretical upper and lower bounds on the maximum number of nodes in a simple flooding mesh network were estimated based on idealized assumptions: perfect synchronization, no collisions, no additional network traffic, no latency, and a static topology. With a transmission time of 1.674 ms per message [20] and a broadcast rate of 1Hz, the maximum number of nodes in a fully connected dense network is estimated to be 24. For a sparse network with nodes in a straight line, the maximum is 199. These calculations illustrate the redundancy in transmissions within a dense network using simple flooding.

Comparison Between Multilateration and WCWCL: The WCWCL algorithm outperforms multilateration, with a mean error of 27 m compared to 35.8 m. Multilateration is also more computationally intensive due to least squares minimization. However, WCWCL cannot localize devices outside the convex hull formed by the receiver nodes, limiting the detection area for spoofing. WCWCL's robustness to changes in transmit power, as shown in Fig. 12, is a significant advantage, unlike multilateration, which is sensitive to transmitter power changes. Both methods are only effective for devices using omnidirectional antennas; directional antennas require a different approach and other algorithms.

Error sources: The localisation experiments were conducted in an unobstructed environment. Any obstructions affecting signal strength will impact location estimates.

Extended range of DRI: DRI messages were successfully transmitted through the FANET over a 1.6 km range. This range is not a limitation of the FANET; theoretically, DRI messages can be extended indefinitely if reliable connections exist between all nodes. However, the FANET implementation does not verify DRI message authenticity, potentially allowing a spoofing device to extend its coverage if within FANET range.

Message Frequency Through the FANET: Fig. 8 shows the frequency at which DRI messages are received by the scanner through the FANET. For the AirPlate, the frequency is ≈ 0.6Hz, which does not meet the DRI standard, although the AirPlate complies with the 1Hz regulation. Message frequency decreases with the number of hops through the network. Reliability can be enhanced by increasing rebroadcasts or the original transmission frequency, as discussed in [20].

Location Estimate of Moving Versus Static Transmitter: The moving transmitter experiment yielded better results than the static one, likely due to a bias-variance tradeoff. Static transmitters might introduce a bias due to misalignment, while the movement of the AirPlate reduces bias but increases variance, which can be mitigated through filtering.

5 CONCLUSION AND FUTURE WORK

To extend the range of DRI messages using a FANET, different broadcast algorithms were evaluated, and simple flooding was found to be the most effective for sparse and dynamic mesh networks. The results confirm that the implemented algorithm effectively extends DRI message range. DRI messages from a quadcopter with an original frequency of 10 Hz were received at $1.5\ Hz$ to $8\ Hz$, while messages from the AirPlate transmitted at 1 Hz were received at approximately $0.6\ Hz$. The experiment also confirmed successful DRI and Mavlink integration.

For DRI message spoofing, two RSSI localisation methods were tested. The WCWCL method proved more favourable than multilateration, as it is robust to changes in transmitter power and does not require reference measurements. Although both methods showed significant localisation errors, WCWCL provided a reasonable estimate of a moving DRI transmitter using a moving average.

Future work includes: 1) adding fields to the DRI payload for hop counter, RSSI, location from the first forwarding node, and authentication signatures; 2) equipping a UAV with an ADS-B receiver to enhance awareness of nearby aircraft; 3) extending localization to 3D by arranging the receiver network in different planes; 4) implementing a hybrid localization approach with both omnidirectional and directional antennas to allow WCWCL to determine if a transmitter is outside the receiver network's convex hull; and 5) developing a self-calibration method where receiving antennas routinely broadcast fixed-power messages to improve accuracy and reduce variance from external disturbances like weather.

ACKNOWLEDGEMENTS

The authors thank August Ravn Mader and Troels Dupont Andreasen from Airplate [22] for their collaboration and for providing the DRI device used in the experiments. This work was supported by the **WildDrone MSCA Doctoral Network**

http://www.imavs.org/

[28] funded by EU Horizon Europe under grant agreement #101071224 and the 5G ENabled communication Infrastructure for Unmanned Aerial System (GENIUS) project [25].

REFERENCES

[1] May 2019. Commission Implementing Regulation (EU) 2019/947 of 24 May 2019 on the rules and procedures for the operation of unmanned aircraft, http://data.europa.eu/eli/reg_impl/2019/947/oj/eng.

[2] Aerospace series - unmanned aircraft systems - part 002: Direct remote identification. Technical report, European Comittee For Standardization, 2023.

[3] ASD-STAN. Introduction to the European UAS Digital Remote ID Technical Standard.

[4] Internet Engineering Task Force Drone Remote ID Protocol.

[5] Drone Remote ID Protocol. datatracker.ietf.org/group/drip/about/.

[6] Christopher Ho et al. Flooding for reliable multicast in multi-hop ad hoc networks. In *Proceedings of the 3rd international workshop on Discrete algorithms and methods for mobile computing and communications*, pages 64–71, Seattle Washington USA, August 1999. ACM.

[7] Sze-Yao Ni et al. The broadcast storm problem in a mobile ad hoc network. In *Proceedings of the 5th annual ACM/IEEE international conference on Mobile computing and networking*, pages 151–162, Seattle Washington USA, August 1999. ACM.

[8] Wei Peng. On the reduction of broadcast redundancy in mobile ad hoc networks. In *2000 First Annual Workshop on Mobile and Ad Hoc Networking and Computing. MobiHOC (Cat. No.00EX444)*, pages 129–130, Boston, MA, USA, 2000. IEEE.

[9] A. Qayyum et al. Multipoint relaying for flooding broadcast messages in mobile wireless networks. In *Proceedings of the 35th Annual Hawaii International Conference on System Sciences*, pages 3866–3875, Big Island, HI, USA, 2002. IEEE Comput. Soc.

[10] Wei Peng. AHBP: An efficient broadcast protocol for mobile Ad hoc networks. *Journal of Computer Science and Technology*, 16(2):114–125, March 2001.

[11] Brad Williams. Comparison of broadcasting techniques for mobile ad hoc networks. In *Proceedings of the 3rd ACM international symposium on Mobile ad hoc networking & computing*, MobiHoc '02, pages 194–205, New York, NY, USA, June 2002. Association for Computing Machinery.

[12] Asma Mesmoudi et al. Wireless Sensor Networks Localization Algorithms: A Comprehensive Survey. *International journal of Computer Networks & Communications*, 5(6):45–64, November 2013.

[13] Guangjie Han et al. Localization algorithms of Wireless Sensor Networks: a survey. *Telecommunication Systems*, 52(4):2419–2436, April 2013.

[14] Tashnim J.S. Chowdhury et al. Advances on localization techniques for wireless sensor networks: A survey. *Computer Networks*, 110:284–305, December 2016.

[15] Bo Yang et al. A Novel Trilateration Algorithm for RSSI-Based Indoor Localization. *IEEE Sensors Journal*, 20(14):8164–8172, July 2020.

[16] Xiuyan Zhu. RSSI-based Algorithm for Indoor Localization. *Communications and Network*, 05(02):37–42, 2013.

[17] J. Blumenthal et al. Precise Positioning with a Low Complexity Algorithm in Ad hoc Wireless Sensor Networks. *PIK - Praxis der Informationsverarbeitung und Kommunikation*, 28(2):80–85, June 2005.

[18] Quande Dong. A Novel Weighted Centroid Localization Algorithm Based on RSSI for an Outdoor Environment. *Journal of Communications*, 9(3):279–285, 2014.

[19] Seeed Studio. https://wiki.seeedstudio.com/XIAO_ESP32C3_Getting_Started/, 2024-06-13.

[20] Høffer, Mads Fogh and Herlev, Victor Dahl. Extending direct remote id reception coverage through ad-hoc mesh networking to improve airspace situational awareness. Master's thesis at University of Southern Denmark.

[21] MAVLink Developer Guide, https://mavlink.io/en/.

[22] AirPlate, https://airplate.dk/.

[23] PX4, https://px4.io/.

[24] QGroundControl. http://qgroundcontrol.com/.

[25] GENIUS. "https://genius.aero/".

[26] DRI relay experiment QGroundControl view. https://youtu.be/CdmBHrqAA-k.

[27] W1039B030 Datasheet. Pulse electronics, https://productfinder.pulseelectronics.com/api/open/part-attachments/datasheet/W1039B030.

[28] WildDrone, https://wilddrone.eu/.

http://www.imavs.org/